

# Theoretical Investigation of the Formation Mechanism of Metallofullerene $Y@C_{82}$

Li-Hua Gan, Chun-Ru Wang\*

*Institute of Chemistry, Chinese Academy of Sciences, Beijing 100080, China*

*Received: October 22, 2004; In Final Form: February 26, 2005*

The formation mechanism of metallofullerene  $Y@C_{82}$  was investigated by ab initio calculations with two theoretical models. The first model is a traditional  $Y@C_{80} + C_2$  “fullerene-road” growing mechanism, in which the  $Y@C_{82}$  is assumed to form by combining  $Y@C_{80}$  and  $C_2$  fragments, and the second model involves formation by an unclosed  $C_{76}$  and a  $C_6Y$  fragment. The calculated results showed that the second mechanism is much more energetically favorable.

## Introduction

$C_{60}$  and other fullerenes are usually formed in high-temperature carbon plasma by arc discharging method or laser vaporizing method in helium atmosphere.<sup>1,2</sup> There have been several models being presented to interpret the fullerene formation mechanism, e.g., fullerenes assemblage from graphite sheets,<sup>3</sup> fullerenes assemblage from clusters,<sup>4</sup> the Nautilus model,<sup>5,6</sup> the fullerene road,<sup>7</sup> crystallization from a liquid cluster,<sup>8</sup> and so on.

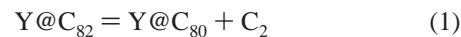
For endohedral fullerenes, due to the involvement of some heteroatoms inside fullerene cages, the formation mechanism becomes more complicated. The production of endohedral fullerenes is usually through two methods experimentally. The first one is through introducing heteroatoms into the existing fullerene cages.<sup>9–15</sup> For example, inert gas atomic endohedral fullerenes  $He@C_{60}/Ne@C_{60}$  can be produced at He/Ne atmosphere under high pressure,<sup>11–13</sup> and  $Li@C_{60}$ ,  $N@C_{60}$  are formed by high-energy ion bombardment.<sup>14,15</sup> In the endohedral fullerene formation process by this mechanism, small atoms or ions such as  $H^+$ , He may directly penetrate through pentagonal or hexagonal rings of fullerene and stay inside the fullerene cage to form endohedral structures.<sup>10</sup> For large atoms/ions such as nitrogen and phosphor, the five- or six-membered rings of fullerene are too small to allow them to pass through the fullerene cage; thus, before the atom/ion insertion several C–C bonds of fullerenes should be broken to create a large opening and reclose afterward.

The second method to produce endohedral fullerenes is through vaporizing graphite/metal composite rods in helium atmosphere.<sup>1,2</sup> Although most endohedral metallofullerenes isolated so far have been produced by this method, their formation mechanism was rarely reported in the literature. An ab initio study had indicated that endohedral metallofullerene containing a large encaged atom cannot be formed through atom/ion insertion or windowing mechanisms as mentioned above,<sup>16</sup> so here we take the  $Y@C_{82}$  as an example and present a hole-repairing formation mechanism of endohedral fullerenes. The model supposes the metallofullerenes to be formed by combining one large unclosed fullerene cluster and a small cluster, and two fragment-combining mechanisms are considered; i.e., the metallofullerene  $Y@C_{82}$  is formed by  $Y@C_{80} + C_2$  or  $C_{76} +$

$C_6Y$ . In both cases the large clusters are unclosed fullerene cages and the small clusters are assumed to repair the holes subsequently. The calculated results demonstrate that the second hole-repairing process, i.e., the  $C_{76} + C_6Y$  mechanism, is more energetically favorable.

## Details of Calculations

The Gaussian 98 program package<sup>17</sup> was employed in calculations.  $Y@C_{82}$  was considered to grow on the basis of either of the following processes



The structures of all these fragments, i.e.,  $Y@C_{80}$ ,  $C_{76}$ ,  $YC_6$ , and  $C_2$ , as well as that of  $Y@C_{82}$  were optimized at the HF/3-21G\* level, and then the chemical reactions were simulated by changing the distances of each pair of fragments ( $Y@C_{80}/C_2$  and  $C_{76}/YC_6$ ). For simplicity we supposed that the structures of all fragments are frozen in reactions, and their relative orientations are also fixed. The total energies at each point along the reaction paths were calculated with a density function theory method (B3LYP) with the basis sets of LANL2DZ<sup>18</sup> for yttrium atom and 3-21G\* for carbon atoms.

Besides the energy criterion, frequency analysis provides also information about molecular stability. Since the frequency calculations of  $Y@C_{82}$  at the HF level are extremely heavy, we adopted a molecular mechanics method (universal force field, UFF)<sup>19</sup> to calculate the vibrational frequencies of the relevant structure of  $Y@C_{82}$ . This method had been used to investigate the vibrational properties of double-walled nanotubes recently and proven to be successful.<sup>24</sup>

## Results and Discussion

**3.1.  $Y@C_{80} + C_2$  Mechanism.** The  $Y@C_{82} = Y@C_{80} + C_2$  formation mechanism is based on the traditional “fullerene-road”<sup>7</sup> formation mechanism, which suggests that a fullerene grows by adding  $C_2$  subsequently. As shown in Figure 1, it is assumed that an unclosed  $C_{80}$  is first formed in the high-temperature plasma by arc-discharging graphite and then the  $C_{80}$  captures an yttrium atom into the cage. Finally, the  $Y@C_{80}$  reacts with a  $C_2$  cluster to repair the opening and form the metallofullerene  $Y@C_{82}$ . The optimized structure of the un-

\* Corresponding author. Telephone: 86-10-62652120. E-mail: crwang@iccas.ac.cn.

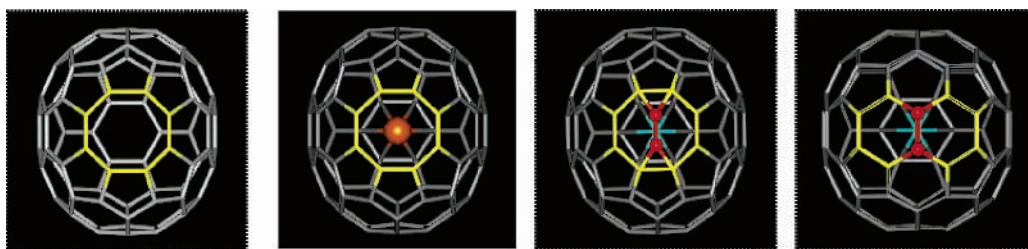


**Figure 1.** Optimized structures of (a) C<sub>80</sub>, (b) Y@C<sub>80</sub>, (c) C<sub>2</sub> + Y@C<sub>80</sub>, and (d) Y@C<sub>82</sub>. Y@C<sub>82</sub> is assumed to form from C<sub>80</sub> by capturing an yttrium atom and a C<sub>2</sub> cluster subsequently.

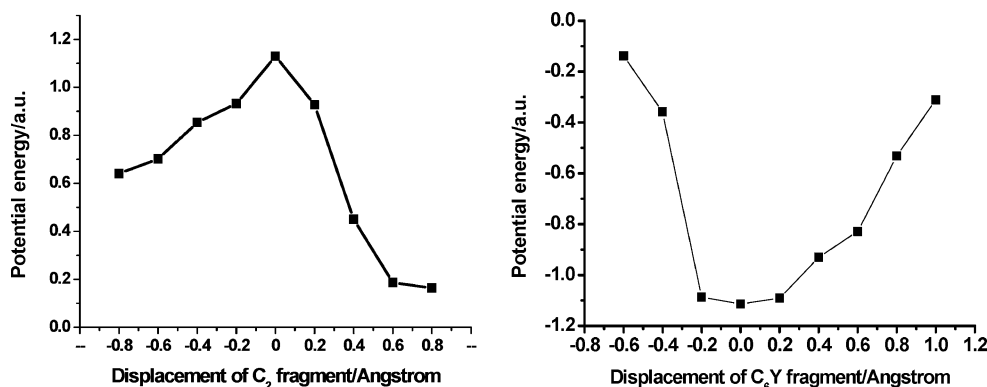


**Figure 2.** Calculated total energies for the two proposed metallofullerene formation mechanisms: (a) Y@C<sub>82</sub> = Y@C<sub>80</sub> + C<sub>2</sub> mechanism; (b) C<sub>6</sub>Y + C<sub>76</sub> mechanism. In both cases the zero point in the abscissa axis is defined as the place where the small fragments (C<sub>2</sub>, C<sub>6</sub>Y) repair the opening of the large fragments (Y@C<sub>80</sub>, C<sub>76</sub>) and form a whole fullerene cage, so the minus value of distances means that the small fragments come into the interior of the large fragments through the opening.

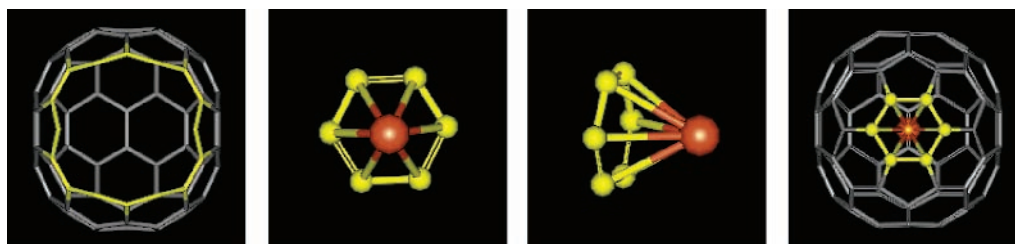
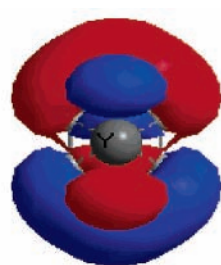
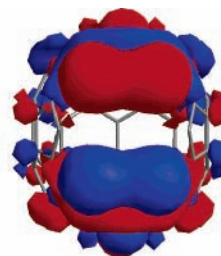
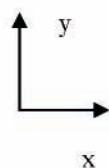


**Figure 3.** Optimized structures of (a) C<sub>76</sub>, (b) C<sub>6</sub>Y (top view), (c) C<sub>6</sub>Y (side view), and (d) Y@C<sub>82</sub>. Y@C<sub>82</sub> is assumed to form by combining C<sub>76</sub> and C<sub>6</sub>Y fragments.



a. HOMO of C<sub>6</sub>Y fragment ( $E_{b2} = -7.9$  eV)



b. LUMO of C<sub>76</sub> ( $E_{b2} = -5.2$  eV)

**Figure 4.** Frontier orbitals of the fragments C<sub>6</sub>Y and C<sub>76</sub>.

closed C<sub>80</sub> has an eight-membered carbon ring, and the yttrium atom locates at the interior of C<sub>80</sub> along the C<sub>2</sub> axis perpendicular to the eight-membered ring plane. To simulate the reaction process of Y@C<sub>80</sub> + C<sub>2</sub>, a C<sub>2</sub> cluster was set to approach Y@C<sub>80</sub> along their shared C<sub>2</sub> axis. A series of single-point energy calculations along the reaction path were performed at the B3LYP/3-21G\*(C)/LANL2DZ(Y) level, and the calculated results are shown in Figure 2a. If we defined the point at which C<sub>2</sub> is reaching the eight-membered ring plane of Y@C<sub>80</sub> as the zero point of the energy curve, it is found that the total energy of Y@C<sub>80</sub> + C<sub>2</sub> increases along the C<sub>2</sub> approaching Y@C<sub>80</sub> and reaches the peak at the zero point where C<sub>2</sub> repairs Y@C<sub>80</sub>

to form Y@C<sub>82</sub> and then dramatically decreases after the C<sub>2</sub> has gone over the zero point to the interior of the fullerene cage. Obviously, the calculation results indicate that the Y@C<sub>80</sub> + C<sub>2</sub> reaction would lead to the Y@C<sub>80</sub> encapsulating C<sub>2</sub> by overcoming an energy barrier of ca. 700 kcal/mol. The endohedral structure Y@C<sub>82</sub> is at the energetic maximum position in the reaction path; thus, it is an unstable structure. Frequency analyses of the Y@C<sub>82</sub> structure reveal one imaginary frequency, confirming that this is not a stable structure.

**3.2. C<sub>76</sub> + C<sub>6</sub>Y Mechanism.** Since the Y@C<sub>80</sub> + C<sub>2</sub> mechanism is not an energetically favorable reaction path for metallofullerene Y@C<sub>82</sub>, we alternately consider the reaction

path of  $C_{76} + C_6Y$ . In fact, it had been shown experimentally a strong correlation between the existence of  $MC_n$  ( $n > 4$ ) and the formation of  $M@C_{82}$ ,<sup>20</sup> and a recent experiment on laser ablation of  $La@C_{82}$  confirmed the high stability of the  $C_6La^+$  cluster.<sup>22</sup> Therefore, it is reasonable to assume that  $C_6Y$  is the main brick in building metallofullerene  $Y@C_{82}$  together with a large-fragment  $C_{76}$ .

A previous molecular dynamics study<sup>23</sup> indicated that the structure of  $C_6M$  is composed of a hexagon ring with a metal atom attached; here we take this structure of  $C_6Y$  as the initial reactant and the unclosed  $C_{76}$  with a 16-membered ring opening as another reactant to fit the large size of  $C_6Y$ . Geometrical optimizations were performed for  $C_{76}$  and  $C_6Y$  fragments, and their optimized structures are shown in Figure 3a–c. Similar to the study in mechanism (1),  $C_6Y$  was assumed to approach  $C_{76}$  along their common  $C_2$  axis, and the point where the hexagon of  $C_6Y$  overlaps with the 16-membered ring of  $C_{76}$  was set as the zero point of the energy curve. As shown in Figure 2b, a series of single-point energy calculations of  $C_{76} + C_6Y$  were performed along the reaction path at the B3LYP/3-21G\*(C)/LANL2DZ(Y) level. Contrary to the  $Y@C_{80} + C_2$  reaction path in which the highest energy appears at the zero point of the energy curve, it was found that the calculated energy of  $C_{76} + C_6Y$  decreases along with the  $C_6Y$  fragment approaching  $C_{76}$  at first, reaches the lowest point at the zero point, and then rapidly increases after  $C_6Y$  going over the zero point to the interior of the  $C_{76}$  cage. Obviously, endohedral metallofullerene  $Y@C_{82}$  is formed at the zero point of the energy curve, where the six-membered ring of  $C_6Y$  merges to the  $C_{76}$  cage, so  $Y@C_{82}$  produced by this mechanism has the lowest energy in the reaction path and is energetically favorable. Frequency analyses on this structure find no imaginary frequencies, confirming that the  $Y@C_{82}$  is an energetic minimum.

The frontier orbitals of  $C_{76}$  and  $C_6Y$  were also calculated as shown in Figure 4. Obviously, the highest occupied molecular orbital (HOMO,  $E_{b2} = -7.9$  eV) of  $C_6Y$  and the lowest unoccupied orbital (LUMO,  $E_{b2} = -5.2$  eV) of  $C_{76}$  are both symmetrically and energetically matched. The reaction of them would lead to electron transfers from the HOMO of  $C_6Y$  to the LUMO of  $C_{76}$ . Mulliken electron analysis demonstrates that the  $C_6Y$  donates 1.2 electrons to  $C_{76}$  in this reaction.

In conclusion, we have proposed two formation mechanisms of  $Y@C_{82}$  under the hole-repairing model. Both energetic calculations and frequency analyses exclude the “fullerene-road” mechanism and support the  $C_{76} + C_6Y$  growing mechanism, indicating that the involvement of metal atoms would affect the fullerene formation process seriously. This may be the reason why empty fullerenes distribute in a large size range from  $C_{60}$  to  $C_{120}$ , but metallofullerenes were only found on certain structures such as  $M@C_{82}$ ,  $M@C_{84}$ .

The  $C_{76} + C_6Y$  growing mechanism explains the formation of  $Y@C_{82}$  very well; however, it should be noted that for other metallofullerenes  $M@C_{82}$  it may be an oversimplified supposition to frozen the fragmental structures while simulating the

reaction path. In reality, the metal ion would adjust its equilibrium position accompanying with charge transfers from  $C_6M$  to  $C_{76}$  in the formation of  $M@C_{82}$ . For example, for some lanthanide metallofullerenes such as  $Gd@C_{82}$ , the Gd ion even moves far from the six-membered ring and close to its opposite C–C bond inside the  $C_{82}$  cage.<sup>25</sup>

**Acknowledgment.** We thank Prof. C.L. Bai for in-depth discussions. Financial support from the National Natural Science Foundation of China (Grant Nos. 90206045 and 50225206), the National Key Project on Basic Research (Grant No. G2000077501), and the Chinese Academy of Sciences are gratefully acknowledged.

## References and Notes

- (1) (a) Kraetschmer, W.; Fostiropoulos, K.; Lamb, L. D.; Huffman, D. R. *Nature* **1990**, 347, 354. (b) Shinohara, H. *Rep. Prog. Phys.* **2000**, 63, 843.
- (2) Chai, Y.; Guo, T.; Jin, C.; Haufler, R. E.; Chibante, L. P. F.; Fure, J.; Wang, L.; Alford, J. M.; Smalley, R. E. *J. Phys. Chem.* **1991**, 95, 7564.
- (3) Heath, J. R.; O'Brien, S. C.; Zhang, Q.; Liu, Y.; Curl, R. F.; Tittel, F. K.; Smalley, R. E. *J. Am. Chem. Soc.* **1985**, 107, 7779.
- (4) (a) Chang, T.-M.; Naim, A.; Ahmed, S. N.; Goodloe, G.; Shevlin, P. B. *J. Am. Chem. Soc.* **1992**, 114, 7603. (b) Goeres, A.; Sedlmayr, E. *Chem. Phys. Lett.* **1991**, 184, 310. (c) Wakabayashi, T.; Achiba, Y. *Chem. Phys. Lett.* **1992**, 190, 465. (d) Wakabayashi, T.; Shiromaru, H.; Kikuchi, K.; Achiba, Y. *Chem. Phys. Lett.* **1993**, 201, 470. (e) Dias, J. R. *Chem. Phys. Lett.* **1993**, 209, 439.
- (5) Zhang, Q. L.; O'Brien, S. C.; Heath, J. R.; Liu, Y.; Curl, R. F.; Kroto, H. W.; Smalley, R. E. *J. Phys. Chem.* **1986**, 90, 525.
- (6) Kroto, H. W.; McKay, K. *Nature* **1988**, 331, 328.
- (7) Heath, J. R. In *Fullerenes: Synthesis, Properties and Chemistry of Large Carbon Clusters*; Hammond, G. S. I., Kuck, V. J., Eds.; American Chemical Society: Washington, DC, 1991; pp 1–23.
- (8) Jing, X.; Chelikowsky, J. R. *Phys. Rev. B* **1992**, 46, 5028–503201. Lozovik, Yu E.; Popov, A. M. *Phys.-Usp.* **1997**, 40, 717.
- (9) Tellgmann, R.; Krawez, N.; Lin, S. H.; Hertel, I. V.; Campbell, E. B. *Nature* **1996**, 382, 407.
- (10) Saunders, M.; Cross, R. J.; Jiménez-Vázquez, H. A.; Shimshi, R.; Khong, A. *Science* **1996**, 271, 1693.
- (11) Kusch, Ch; Krawez, N.; Tellgmann, R.; Winter, B.; Campbell, E. B. *Appl. Phys. A* **1998**, 66, 293.
- (12) Mauser, H.; Hommrd N. van E.; Clark, T.; Hirsch, A.; Pietzak, B.; Weidinger, A.; Dunsch, L. *Angew. Chem., Int. Ed. Engl.* **1997**, 36, 2835.
- (13) Saunders, M.; Jimenez-Vazquez, H. A.; Cross, R. J.; Poreda, R. J. *Science* **1993**, 259, 1428.
- (14) Murphy, T. A.; Pawlik, T.; Weidinger, A.; Hoehne, M.; Alcalá, R.; Spaeth, J. M. *Phys. Rev. Lett.* **1996**, 77, 1075.
- (15) Knapp, C.; Dinse, K.-P.; Pietzak, B.; Waiblinger, M.; Weidinger, A. *Chem. Phys. Lett.* **1997**, 272, 433.
- (16) Sanville, E.; BelBruno, J. J. *J. Phys. Chem. B* **2003**, 107, 8884.
- (17) Frisch, M. J.; et al. *Gaussian 98*; Gaussian: Pittsburgh, PA, 1998.
- (18) Hay, P. J.; Wadt, W. R. *J. Chem. Phys.* **1985**, 82, 299.
- (19) Rappe, A. K.; Casewit, C. J.; Colwell, K. S.; Goddard, W. A.; Skiff, W. M. *J. Am. Chem. Soc.* **1992**, 114, 10024.
- (20) Suzuki, S.; Torisu, H.; Kubota, H.; Wakabayashi, T.; Shiromaru, H.; Achiba, Y. *Int. J. Mass Spectrom. Ion Processes* **1994**, 138, 297.
- (21) Murry, R. L.; Scuseria, G. E. *Science* **1994**, 263, 791.
- (22) Lassesson, A.; Gromov, A.; Mehlig, K.; Taninaka, A.; Shinohara, H.; Campbell, E. B. *J. Chem. Phys.* **2003**, 119, 5591.
- (23) Yamaguchi, Y.; Maruyama, S. *Eur. Phys. J. D* **1999**, 9, 385.
- (24) Yao, N.; Lordi, V. *Phys. Rev. B* **1998**, 58, 12649.
- (25) Nishibori, E.; Iwata, K.; Sakata, M.; Takata, M.; Tanaka, H.; Kato, H.; Shinohara, H. *Phys. Rev. B* **2004**, 69, 113412.